Appl. Phys. B 83, 295–301 (2006)
DOI: 10.1007/s00340-006-2146-9

Applied Physics B
Lasers and Optics

W.X. QUE[1,✉]
W.G. LIU[2]
X. HU[3]

Preparation and optical properties of sol–gel neodymium-doped germania/γ-glycidoxypropyltrimethoxysilane organic–inorganic hybrid thin films

[1] Electronic Materials Research Laboratory, Xi'an Jiaotong University, Xi'an 710049, Shaanxi, P.R. China
[2] Micro-optoelectronic Systems Laboratories, Xi'an Institute of Technology, Xi'an 710032, Shaanxi, P.R. China
[3] School of Materials Science and Engineering, Nanyang Technological University, Nanyang Avenue, Singapore 639798, Singapore

Received: 31 August 2005/Final version: 17 January 2006
Published online: 29 March 2006 •

ABSTRACT Germania/γ-glycidoxypropyltrimethoxysilane organic–inorganic hybrid spin-coating thin films doped with neodymium ions are prepared by a sol–gel technique and a spin-coating process. Acid-catalyzed solutions of γ-glycidoxypropyltrimethoxysilane mixed with germanium isopropoxide are used as matrix precursors. Thermal gravimetric analysis, UV–visible spectroscopy, and Fourier transform infrared spectroscopy are used to study the structural and optical properties of the hybrid thin films. The results indicate that films that are crack-free and have a high transparency in the visible and near-infrared range can be obtained; a strong UV absorption region at short wavelength ~ 200 nm, accompanied with a shoulder peaked at ~ 240 nm, due to the neutral oxygen monovacancy defects, is also identified. Upconversion emission properties of the transparent dried gel and the thin films heated at different heat treatment temperatures and doped with different neodymium ion concentrations are studied; a relatively strong room-temperature yellow to violet upconversion emission at 397 nm ($^4D_{3/2} \rightarrow {}^4I_{13/2}$) is observed under a xenon lamp excitation with yellow light at the wavelength of 580 nm ($^4I_{9/2} \rightarrow {}^4G_{5/2}$). The effect of Nd^{3+} doping concentration and heat treatment temperature on upconversion emission of the thin films is also studied. The mechanism of the upconversion is proposed.

PACS 81.05.Kf; 81.20.Fw; 78.55.Hx

1 Introduction

The study of the upconversion in rare-earth-doped new host materials has recently attracted much interest [1–3]. Especially, the availability of high-power infrared laser diodes has stimulated researches in the areas of upconversion pumped visible lasers and the potential applications in the areas such as three-dimensional displays, high-density optical data reading and storage, and infrared laser viewers and indicators [4–6], among many. It is well known that rare earths such as neodymium have already proven to be very useful in photonics for the construction of a laser system due to their four-level energy structure, which is more ideal for the laser transition. GeO_2-based systems are photosensitive and can be employed for the formation of photorefractive Bragg gratings and second-harmonic generation, and GeO_2–SiO_2 has been recognized as being excellent for obtaining optical waveguide films with controllable refractive index [7] as well as a large concentration doping of rare-earth ions [8, 9]. A number of research groups have reported progress in such material systems doped with rare-earth ions by the sol–gel route [10–15]. However, as these reported material systems generally employ tetraethylorthosilicate as a SiO_2 source, the heat treatment temperature needs to be quite high (around 1000 °C). Therefore, it is very difficult to produce a film thicker than 0.2 μm by a single-coating process and it is impossible for them to integrate with semiconductor sources and detectors directly. An attractive way to overcome these problems is the use of organically modified silane (ormosil) precursors that can produce a relatively thick single-coating layer at a low temperature or even room temperature [16–18]. Moreover, the moderate processing temperatures can enable direct integration on the same chip with semiconductor sources and other optoelectronic components. Due to these promising advantages, it is interesting to study GeO_2/ormosil organic–inorganic hybrid materials doped with rare-earth ions for photonic applications. However, there have been few reports on the preparation and optical properties of the sol–gel-derived GeO_2/ormosil organic–inorganic hybrid materials doped with rare-earth ions so far.

In this work, we report our recent study on the preparation, characterization, and optical properties of the neodymium-doped germania/γ-glycidoxypropyltrimethoxysilane hybrid thin films obtained at different heat treatment temperatures and the corresponding transparent dried gel glass. In addition, we also report the effects of the heat treatment temperature and doping concentration of neodymium ions on upconversion emission properties of the thin films by thermal gravimetric analysis, UV–visible spectroscopy, and Fourier transform infrared spectroscopy.

2 Experimental

A neodymium-doped germania/γ-glycidoxypropyltrimethoxysilane hybrid thin film sol and its transparent dried gel glass were prepared by a sol–gel technique from an organic–inorganic hybrid system. Germanium isopropoxide

✉ Fax: +86-29-82668794, E-mail: wxque@mail.xjtu.edu.cn

(TEOG, $Ge[OCH(CH_3)_2]_4$) and γ-glycidoxypropyltrimethoxysilane (GLYMO, $(CH_2OCH)CH_2O(CH_2)_3Si(OCH_3)_3$) were used as precursors for germania (GeO_2) and ormosil resources, respectively. Hydrochloric acid (HCl, 37 wt. % in water) was used as catalyst, 2-methoxyethanol ($CH_3OCH_2CH_2OH$) as chelating agent of TEOG, ethanol as solvent, and de-ionized water for hydrolysis. In the preparation of the GeO_2/GLYMO hybrid sol, GLYMO was dissolved in ethanol and pre-hydrolyzed with de-ionized water and hydrochloric acid. The solution was stirred for an hour. Germanium isopropoxide was added to 2-methoxyethanol ($CH_3OCH_2CH_2OH$) under a dry nitrogen environment and the solution was agitated until homogenization was reached. Then, the two solutions were mixed with a molar ratio of 30 : 70 (TEOG to GLYMO). Neodymium nitrate was dissolved in ethanol and added drop-by-drop to the 30 GeO_2–70 GLYMO solution to obtain sols with an $Nd/(GeO_2 + GLYMO)$ molar concentration of 0.2, 0.5, and 1 mol % Nd^{3+}, respectively. The final mixture was stirred for about 50 h at room temperature. Following the common practice for spin coating, a 0.1 micron pore filter was attached to a syringe for removing foreign particles before the resultant solution was spin coated onto a substrate. The substrates including quartz and silicon were used in our experiment. One layer of the sol–gel thin film was spun onto the substrate at 3500 rpm for 30 s. The film-coated samples were then heated for 10 min at different temperatures of 100, 200, 300, 400, 500, and 600 °C. In order to obtain a dried gel glass, the resulting sol was poured into a Petri dish and put at room temperature for about two weeks and then kept at 100 °C for one week so as to obtain a transparent dried gel. The gel obtained was approximately 2 mm in thickness. It should be mentioned here that all reactions and manipulations were carried out under a dry nitrogen environment due to the extreme moisture sensitivity of the germanium alkoxides.

Neodymium-doped GeO_2/GLYMO hybrid thin films (or transparent dried gels) were characterized by thermal gravimetric analysis (TGA), UV–visible spectroscopy (UV-VIS), and Fourier transform infrared spectroscopy (FTIR). A Perkin-Elmer 7 Series was used for TGA measurement of the gel powders obtained from the corresponding solutions, which was done at a heating rate of 5 °C/min in a flowing nitrogen gas environment. The UV–visible absorption spectra were measured for the thin films deposited on quartz in the range of 200–1000 nm on a UV-VIS spectrometer, which has a resolution of ±0.3 nm. The FTIR spectra of the thin films deposited on silicon substrates were measured in the range of 4000–400 cm^{-1} with a resolution of ±1 cm^{-1}. The thickness and the refractive index of the thin films were measured by an *m*-line apparatus (Metricon 2010) based on a prism coupling technique. The propagation loss was measured by recording the light intensity scattered out of the waveguide plane, which is proportional to the guided intensity. This intensity was recorded by a fiber probe scanning down the length of the propagating streak. These measurements were performed by exciting the transverse electric TE_0 mode of the waveguide with a laser at the wavelength of 1550 nm. The upconversion emission properties of the Nd^{3+}-doped thin film and its corresponding transparent dried gel were measured under a yellow-light excitation of 580 nm on a Spex Fluorolog-3 spectrofluorometer with a 1934D3 phosphorimeter attached. This system employs the Datamax software package to acquire the spectra. The source of excitation is a Xe continuous wavelength (cw) source for the steady state upconversion emission measurement.

3 Results and discussion

The optical waveguide properties of the films such as refractive indices, propagation modes, and loss properties were studied using an *m*-line apparatus based on a prism coupling technique. In order to excite all possible waveguide modes, the phase-matching condition between prism and film needs to be met. This requires the refractive index of the prism to be larger than that of the film. A laser beam is coupled into the film through a prism. The effective mode index (N_m) is calculated by [19]

$$N_m = N_p \sin\left(\sin^{-1}(\sin\theta_m/N_p) + A_p\right) , \quad (1)$$

where N_p is the refractive index of the prism, A_p is its base angle, and θ_m is the incident angle of the laser beam to the prism. In our case, $N_p = 2.1653$ at 633 nm and 2.1227 at 1550 nm, and $A_p = 50.75°$. The film heated at 200 °C was found to support several TE modes at 633 nm, as is shown in Fig. 1. However, considering that the substrate index is about 1.457 for a wavelength of 633 nm, it is evident that only the two highest indices for each polarization are higher than this value, that is to say, only two modes of TE_0 and TE_1 can be guided modes of the waveguide and used for calculating the refractive index and the thickness. The other dips observed in the intensity spectra are substrate modes due to their refractive indices being smaller than the value of the substrate refractive index. The thickness and refractive index of the thin films doped with 0.5 mol % Nd^{3+} and heated at different heat treatment temperatures were estimated. The thin films were spun on silicon substrates by a single spin-coating process. As expected, with increase of the heat treatment temperature, the refractive index of the thin film increases and the thickness drops. That is to say, the film thickness becomes thinner and the refractive index becomes higher as the heat treatment temperature rises. For example, a dense film with a thickness of

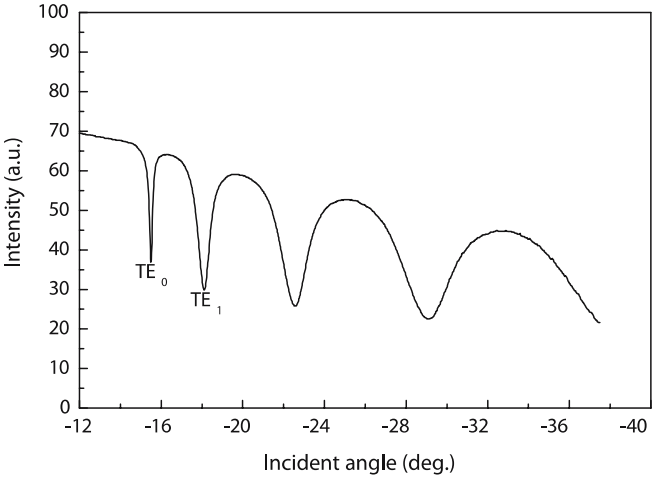

FIGURE 1 Optical guided TE modes of the hybrid waveguide thin film at the wavelength of 633 nm

about 1.80 μm can be obtained by a single spin-coating process at the heat treatment temperature of 100 °C, but the thickness of the thin film drops to about 0.65 μm when the heat treatment temperature was increased to 500 °C. It should be mentioned here that the thickness and refractive index of the thin film are not sensitive to the heat treatment temperature in the range between 100 and 200 °C. For example, the decrease of the film thickness is about 4% and the increase of the refractive index is about 0.1%, respectively, when the heat treatment temperature was increased from 100 to 200 °C. It can also also obtained that within the heat treatment temperature range between 100 and 500 °C, the refractive index of the thin film can be varied from 1.499 to 1.519 at the wavelength of 633 nm.

The optical propagation loss at 1550 nm, for the TE_0 mode, was also evaluated by a scattered-light measurement technique based on fiber photometric detection. The loss was typically 2.4 dB/cm at 1550 nm for the waveguide film heated at 100 °C. It is obvious that the loss of the waveguides prepared at the present process conditions is relatively large as compared to those reported previously for a SiO_2–GeO_2 planar waveguide [20, 21]. The total loss of a planar waveguide consists of absorption and scattering contributions, the latter being usually predominant at the wavelength of interest in integrated optics. The scattering loss for an amorphous waveguide is the sum of two contributions, including surface scattering due to the surface roughness of the film, and volume scattering due to local fluctuations in the refractive index resulting from density and compositional variations. Nonuniform hydrolysis and condensation of the binary alkoxide mixture undoubtedly result in the big scattering loss. The homogeneity of a sol–gel glass synthesized from a mixture of two or more alkoxide precursors is affected by the relative rates of homocondensation and heterocondensation. Silicon alkoxides hydrolyze relatively slowly, and acid or base catalysis is frequently employed to accelerate the reaction. However, germanium alkoxides hydrolyze at a much faster rate; as a result, in mixtures of germanium and silicon alkoxides, it is still possible that a heterogeneous network containing Ge-rich and Si-rich domains is formed in this system [21].

Figure 2 shows the optical transmittance spectra of the hybrid thin films doped with 0.5 mol % Nd^{3+} and deposited on quartz as a function of the heat treatment temperature. Note that these were single-layer thin films. It can be seen that the thin films are transparent and colorless. All the thin films have high transmittance, and the transmittance changes with the heat treatment temperature. For those thin films heated below 400 °C, the transmittance decreases with an increase of the heat treatment temperature from 100 to 400 °C. But, with further increase of the heat treatment temperature, the transmittance of the thin films starts to increase. Based on the results obtained by TGA and FTIR as mentioned below, this behavior can be explained as follows. The thin films heated at a relatively low temperature (below 300 °C) are dense due to the addition of GLYMO, but the thin film heated at 400 °C becomes porous due to the incomplete combustion and decomposition of the organic compounds. As a result, apart from the scattering-like λ^{-4} dependence for Rayleigh scattering, a relatively large degree of scattering of incident light from the pores or the scattering area resulting from the incomplete combustion and decomposition of the organic compounds is

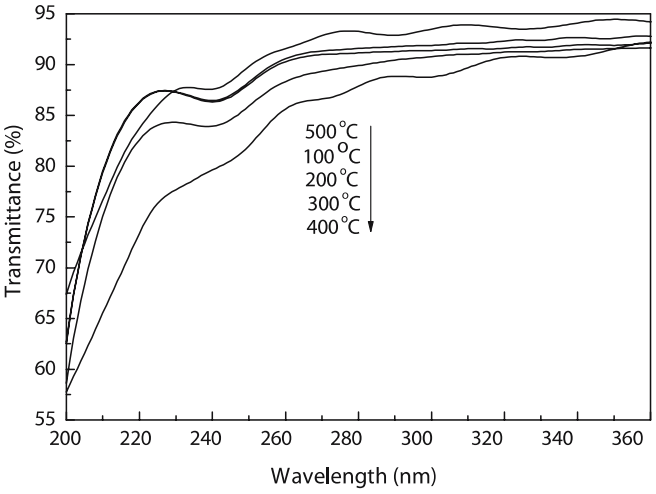

FIGURE 2 Optical transmittance spectra of the thin films as a function of the heat treatment temperature

also expected. However, when the heat treatment temperature further increases to 500 °C or above, the organic compounds would have been completely decomposed or burst and an inorganic GeO_2–SiO_2 thin film is probably formed. Thus, the scattering and absorption from the scattering area due to the incomplete combustion and decomposition of the organic compounds is thus substantially suppressed or even vanishes, also leading to probably the lower porosity (lower scattering) of the thin film as compared with that of the thin film heated at 400 °C. It should be mentioned here for all thin films besides the one heated at 400 °C that a strong UV absorption at short wavelengths $\sim$ 200 nm accompanied with an obvious shoulder absorption located at $\sim$ 240 nm can be clearly observed. There is a consensus over the assignment of the absorption band at around $\sim$ 200 nm to Si E' and Ge E' centers [22, 23]. The absorption at $\sim$ 240 nm is also well characterized and associated with an increase in the concentration of neutral oxygen monovacancy defects [22–26]. For the film heated at 400 °C, there is no obvious $\sim$ 240 nm absorption band observed; an explanation is that the large degree of scattering of incident light by the pores or the scattering area caused by the incomplete combustion and decomposition of the organic compounds covers the $\sim$ 240 nm absorption band. It can be concluded from the UV absorption results that a heat treatment temperature below 300 °C is necessary to attain a dense, low-absorption, and high-transparency sol–gel hybrid thin film by the present process. In order to understand these results well, TGA was employed to characterize the thermal process of the sample.

Figure 3 shows the TGA curve of the gel powder. It can be seen from Fig. 2 that the weight loss occurs at three stages mainly, namely, below 100 °C, between 350 and 450 °C, and from 450 to 520 °C. Below 100 °C, the weight loss is considered to be due to the volatilization and thermal decomposition of the remnant of organic solvents. Between 350 and 450 °C, the weight loss is attributed to the carbonization or combustion of the organic compounds. Between 450 and 520 °C, the weight loss is probably ascribed to the evaporation of physically absorbed water and the further combustion of the organic compounds. As there is no major weight loss afterwards, it

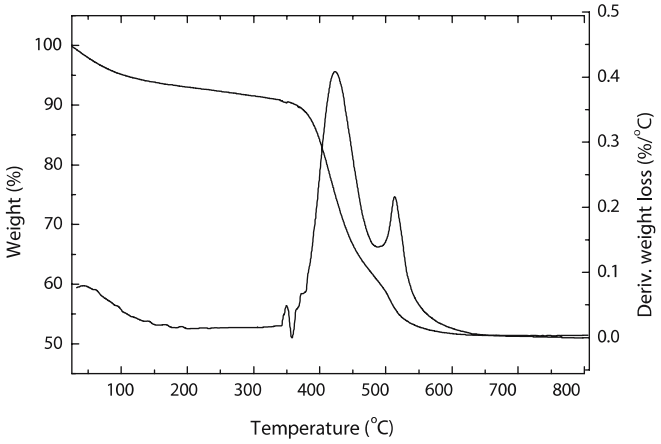

FIGURE 3 TGA curve of gel powder obtained from the solution doped with 0.5 mol % neodymium ions

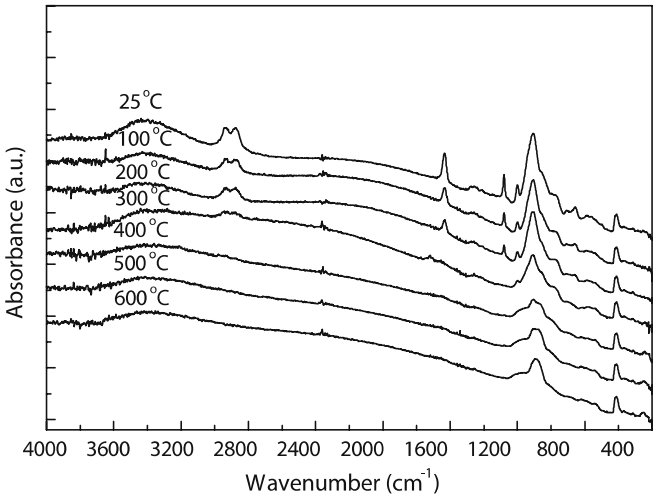

FIGURE 4 FTIR absorption spectra of the thin films doped with 0.5 mol % neodymium ions and heated at different heat treatment temperatures

can be considered that the organic compounds have been completely burnt off and the sample to be inorganic glass. It can be seen clearly from Fig. 3 that the obvious and faster weight loss occurs at the stage between 350 and 450 °C. These results are helpful to understand the results obtained by UV-VIS transmittance spectra, where the film heated at 400 °C shows a relatively low transmittance due to the incomplete combustion and decomposition of the organic compounds. In addition, it can also be noted from the TGA curve that there is no obvious weight loss below a heat treatment temperature of 300 °C; this can be used to understand why the thickness and refractive index of the thin film are not sensitive to the heat treatment below 300 °C as well as why these thin films heated below 300 °C have a relatively high transmittance as compared with that obtained at 400 °C.

Figure 4 shows the FTIR absorption spectra of the thin films doped with 0.5 mol % Nd^{3+} and deposited on the silicon substrates as a function of the heat treatment temperature. The main band peak at 1106 cm^{-1} is assigned to Si–O–R stretching vibrations of O–R groups directly bonded to silicon [27]. This band decreases in intensity with an increase of the heat treatment temperature, which is indicative of a densification of the silicon-oxide skeleton. It can be seen for the thin films heated below the heat treatment temperature of 300 °C that there are two weak peaks at 1200 and 1280 cm^{-1}, which correspond to the $–CH_3$ rocking vibration from $Si–O–CH_3$ functional groups and the vibration of the $Si–CH_3$ bond [28], respectively, and a broad peak centered at 2892 cm^{-1}, which corresponds to the $–CH_2–$ symmetric stretching vibration. These peaks weaken and vanish with the increase of the heat treatment temperature; the weakening or even vanishing is attributed to the burning reaction of the thin films in the densification process. The band at 960 cm^{-1} is attributed to Ge–O–Ge anti-symmetric stretching. The band around 780 cm^{-1} is ascribed to symmetric stretching motions of oxygen atoms along the bisector of the Si–O–Si bridging angle [15]. There is a peak at 1631 cm^{-1} for the films heated at 100 and 200 °C or room temperature, which should be attributed to the H–O–H bending vibration of water. The intensity of this peak becomes weak with increase of the heat treatment temperature and vanishes gradually when the heat treatment temperature was increased to 400 °C or above. Furthermore, a broad band between 3100 cm^{-1} and 3600 cm^{-1} is attributed to the O–H stretching vibration. It should be noted here that a broad OH stretching vibration is observed in all films, but the intensity becomes weak gradually with increase the heat treatment temperature. That is to say, the amount of OH content in the film can be gradually reduced with the increase of the heat treatment temperature, but it is difficult to remove it completely from the thin film, even when the heat treatment temperature was increased to 600 °C. An accurate quantitative calculation of the OH content in our thin films was not made due to the difficulties involved as witnessed by others [7, 10]. The OH sensitivity of our FTIR spectrometer is estimated to be about a few hundred ppm. From the thin film heated at 600 °C in Fig. 4, in short, an increase in the heat treatment temperature leads to a decrease in hydroxyl content. It should be noted that the peak at 600 cm^{-1} observed for all the films is from the silicon substrate.

Figure 5 shows an absorption spectrum of a 0.5 mol % Nd^{3+}-doped GeO_2/GLYMO organic–inorganic hybrid transparent dried gel together with the assigned excited levels of Nd^{3+}. It can be seen that nine absorption bands are observed and assigned to the electronic transitions of $^4I_{9/2} \rightarrow {}^2P_{3/2}$, $^2G_{9/2}$, $^4G_{7/2}$, $^4G_{5/2}$, $^2H_{11/2}$, $^4F_{9/2}$, $^4S_{3/2}$ ($^4F_{7/2}$), $^4F_{5/2}$, and $^3F_{3/2}$. Among these, the $^4I_{9/2} \rightarrow {}^4G_{5/2}$ absorption band (hypersensitive transition which satisfies the selection rules of $\Delta J = \pm 2$, $\Delta L = \pm 2$, and $\Delta = 0$) at about 580 nm is an obviously intense one and hence it was chosen to measure the upconversion emission spectrum of the transparent dried gel.

Figure 6 shows a visible upconversion emission characteristic spectrum in the Nd^{3+}-doped GeO_2/GLYMO organic–inorganic hybrid transparent dried gel under the excitation of 580 nm. It can be seen from Fig. 6 that apart from a bright violet upconversion emission transition at 397 nm corresponding to the $^4D_{3/2} \rightarrow {}^4I_{13/2}$ or $^2P_{3/2} \rightarrow {}^4I_{11/2}$ transition of the neodymium ions, an ultraviolet emission transition at 345 nm ($^4D_{3/2} \rightarrow {}^4I_{9/2}$) and a blue emission transition at 470 nm ($^2P_{3/2} \rightarrow {}^4I_{13/2}$) are also observed. But, it should be noted that an ultraviolet emission at about 370 nm ($^4D_{3/2} \rightarrow {}^4I_{11/2}$ or $^2P_{3/2} \rightarrow {}^4I_{9/2}$) has not been observed. This might be due to an effect from the relatively intense emission at 345 nm;

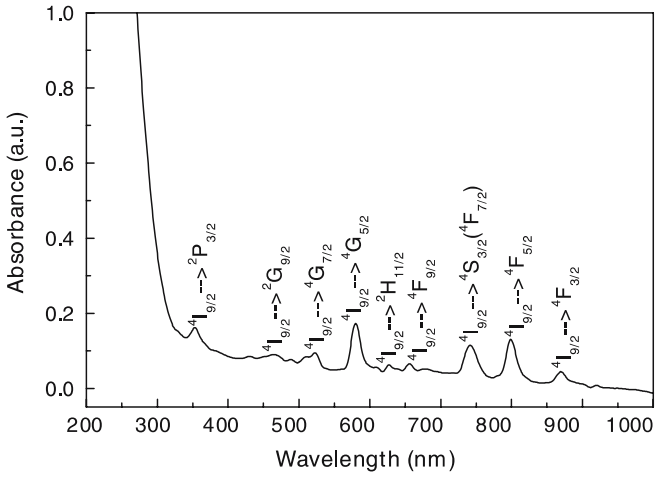

FIGURE 5 Absorption spectrum of the 0.5 mol % Nd^{3+}-doped GeO_2/GLYMO transparent dried gel

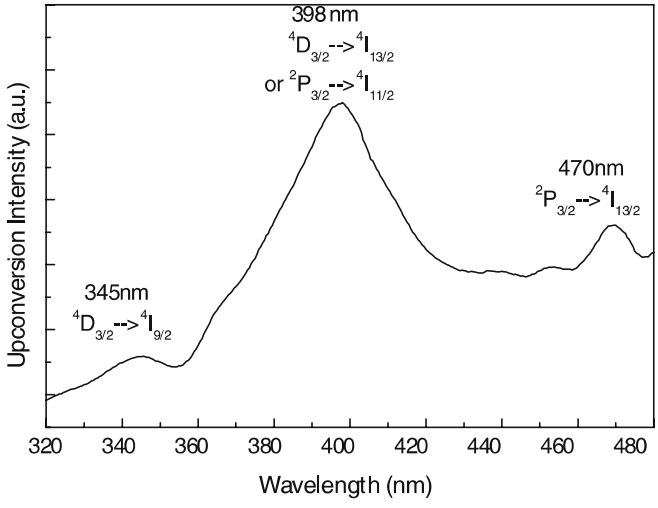

FIGURE 6 Visible upconversion emission spectrum in the 0.5 mol % Nd^{3+}-doped GeO_2/GLYMO transparent dried gel under the excitation of 580 nm

the weak emission at 370 nm is covered by the relatively intense emission at 345 nm. It should also be mentioned that we know of no other intense upconversion luminescence at 397 nm from the neodymium(III) ion in the gel baked at a low temperature of 100 °C as a result of being induced by a continuous wavelength xenon lamp.

Figure 7 shows the upconversion emission spectra of the thin films with different neodymium ion contents and heated at 500 °C. It should be noted that they are two-layer thin films deposited on quartz. Similarly, apart from a bright violet upconversion emission transition at 397 nm corresponding to the $^4D_{3/2} \rightarrow {}^4I_{13/2}$ or $^2P_{3/2} \rightarrow {}^4I_{11/2}$ transition of the neodymium ions, a relatively weak ultraviolet emission transition at 371 nm and a blue emission transition at 469 nm are also observed, but the emission at 345 nm, which was clearly observed in the transparent dried gel sample, did not appear in these thin-film samples. There is no reasonable explanation for this phenomenon; it is possible that the emission intensity of this peak in thin-film samples is too weak to be observed. It should be mentioned here that the peak position of the emission transitions of the thin-film samples is almost the same

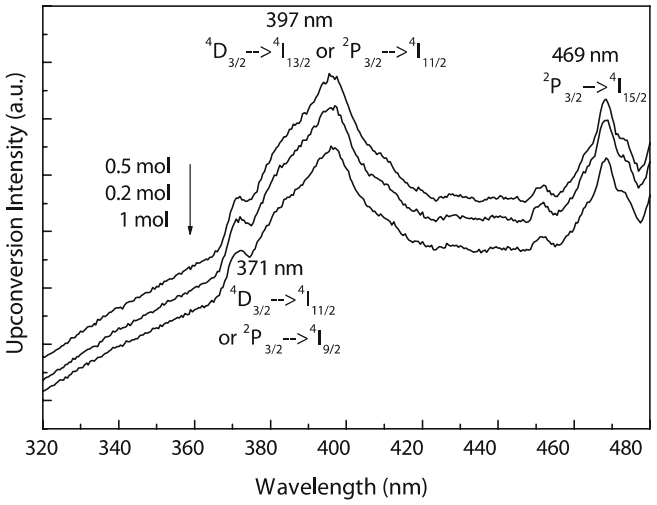

FIGURE 7 Visible upconversion emission spectra from the thin films heated at 500 °C and doped with different neodymium ion concentrations under the excitation of 580 nm

as that of the dried gel sample. It can be observed that the thin film doped with 0.5 mol % Nd^{3+} has the highest intensity of the upconversion emission transition. With an increase of the neodymium ion molar concentration, the upconversion emission intensity first increases and then decreases due to a concentration quenching effect which results from the cross-relaxation process as a result of the reduced inter-ionic distance at higher neodymium ion content; for example, the thin film doped with 1 mol % Nd^{3+} shows the lowest upconversion intensity in all thin films shown in Fig. 7. Figure 8 shows the upconversion emission spectra of the 0.5 mol % Nd^{3+}-doped two-layer films deposited on silicon substrates as a function of the heat treatment temperature. The spectra illustrate clearly that the upconversion emission intensity of the film changes a lot with the heat treatment temperature. However, the peak position and the shape of the spectra are independent of the heat treatment temperature. The upconversion emission intensity of the film heated at 300 °C is the highest of all the films measured, and the film heated at 400 °C shows the lowest upconversion emission intensity. It is probably due to the incomplete combustion and decomposition of the organic compounds at this heat treatment temperature of 400 °C. This is because the incomplete combustion or decomposition of the organic compounds will lead to the appearance of holes inside the thin film, and these holes will cause scattering of light and weaken the emission intensity. Actually, a relatively intense upconversion emission can be observed from the film heated at 500 °C due to a more dense thin film with an increase of the heat treatment temperature. On the other hand, when the heat treatment temperature is low (below 200 °C), a dense thin film can also be obtained due to the addition of the GLYMO; therefore, the thin films heated below 200 °C also show relatively high emission intensity. It should be mentioned here that the emission spectra depicted in Figs. 6–8 exhibit relatively wide emission bands compared to what are observed in crystals or glasses [29–31]; this should be attributed to a remnant of the excitation Xe light passing the filters of the spectrofluorometer. Because it is known that the optical filters used are not quite ideal, this plays a role

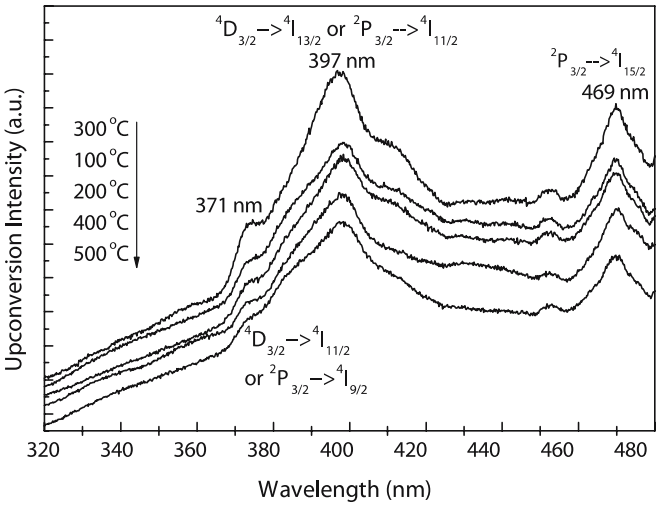

FIGURE 8 Visible upconversion emission spectra from the thin films doped with 0.5 mol % neodymium ion concentration and heated at different heat treatment temperatures under the excitation of 580 nm

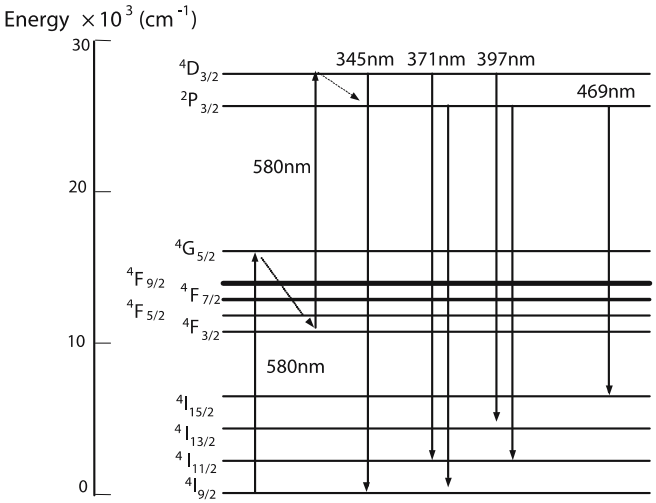

FIGURE 9 Energy level scheme describing the upconversion emission from the Nd^{3+}-doped GeO_2/GLYMO transparent dried gel and thin films upon excitation at 580 nm

when measuring small signals such as rare-earth fluorescence. Actually, Xiang et al. [13] and Annapurna et al. [32] also obtained wide emission bands which are almost the same as that observed in the present paper, since they also employed the same measurement system with a xenon lamp as excitation source.

It is proposed based on the above results and the analysis in Figs. 7 and 8 that a result of a sequential two-photon absorption process including the sequence of ground- and excited-state absorption steps may be responsible for the upconversion process. Figure 9 provides the schematic diagram to explain the mechanism of upconversion emission from a neodymium ion via a sequential two-photon absorption process. In this process, by an initial absorption of a 580-nm photon, an electron from the ground state of $^4I_{9/2}$ first becomes excited to an upper state of $^4G_{5/2}$. Since this state is unstable, the electron rapidly decays non-radiatively to a metastable $^4F_{3/2}$ level. Because this metastable level has a relatively long lifetime, before it further decays, the electron has a good chance to absorb a second 580-nm photon and be excited to the $^4D_{3/2}$ state. Afterwards, some electrons could decay radiatively to the ^4I_J ($J = 11/2, 13/2$, and $15/2$) states, resulting in upconversion emission transitions, or electrons could decay non-radiatively firstly to the $^2P_{3/2}$ state, and then cause other upconversion photon emissions again.

4 Conclusions

Nd^{3+}-doped GeO_2/GLYMO hybrid thin films have been studied for photonic applications by the sol–gel process from organically modified silane precursors. The effects of the heat treatment temperature on optical and structural properties of the thin films have been characterized by TGA, UV-VIS, and FTIR spectroscopy. The results indicate that a heat treatment temperature below 300 °C is expected to produce a dense, low- absorption, high-transparency hybrid thin film. The introduction of ormosil GLYMO provides the advantage of producing thicker films and obtains a dense film at low temperature. A strong UV absorption region at short wavelengths $\sim$ 200 nm, accompanied with a shoulder peaked at $\sim$ 240 nm, due to the neutral oxygen monovacancy defects, has been identified. Upconversion emission luminescence of the transparent dried gel and the thin films heated at different heat treatment temperatures and doped with different Nd^{3+} concentrations have been observed. Experimental results show a strong violet upconversion at 397 nm, a UV emission at 371 nm, and a blue emission at 469 nm. A strong upconversion emission at 345 nm has been observed for the transparent dried gel sample. The sequential two-photon absorption process has been proposed to be responsible for the upconversion mechanism.

ACKNOWLEDGEMENTS This work was supported by the National Natural Science Foundation of China under Grant No. 60477003.

REFERENCES

1 A.S. Gouveia-Neto, E.B. da Costa, L.A. Bueno, S.J.L. Ribeiro, Y. Messaddeq, J. Luminesc. **116**, 52 (2006)
2 D.Q. Chen, Y.S. Wang, Y.L. Yu, E. Ma, F. Bao, Z.J. Hu, Y. Cheng, Mater. Chem. Phys. **95**, 264 (2006)
3 A. Mendioroz, R. Balda, M. Al-Saleh, J. Fernández, Opt. Mater. **27**, 1704 (2005)
4 T. Hebert, R. Wannemacher, W. Lenth, R.M. Macfarlane, Appl. Phys. Lett. **57**, 1727 (1990)
5 E. Downing, L. Hesselink, J. Ralston, R.M. Macfarlane, Science **273**, 1185 (1996)
6 G.S. Maciel, A. Biswas, R. Kapoor, P.N. Prasad, Appl. Phys. Lett. **76**, 1978 (2000)
7 G. Brusatin, M. Guglilmi, A. Martucci, J. Am. Ceram. Soc. **80**, 3139 (1997)
8 M. Benatsou, M. Bouazaoui, Opt. Commun. **137**, 143 (1997)
9 C. Duverger, S. Turrell, M. Bouazaoui, F. Tonelli, M. Montagna, M. Ferrari, Philos. Mag. B **77**, 363 (1998)
10 C. Strohhöfer, S. Capecchi, J. Fick, A. Martucci, G. Brusatin, M. Guglielmi, Thin Solid Films **326**, 99 (1998)
11 K. Kojima, T. Fujita, M. Yamazaki, J. Non-Cryst. Solids **259**, 63 (1999)
12 C. Duverger, M. Ferrari, C. Mazzoleni, M. Montagna, G. Pucker, S. Turrell, J. Non-Cryst. Solids **245**, 129 (1999)
13 Q. Xiang, Y. Zhou, B.S. Ooi, Y.L. Lam, Y.C. Chan, C.H. Kam, Thin Solid Films **370**, 243 (2000)
14 M. Nogami, J. Luminesc. **92**, 329 (2001)
15 A. Martucci, A. Chiasera, M. Montagna, M. Ferrari, J. Non-Cryst. Solids **322**, 295 (2003)

16 H. Schmidt, H. Wolter, J. Non-Cryst. Solids **121**, 428 (1990)
17 D. Shamrakov, R. Reisfeld, Chem. Phys. Lett. **213**, 47 (1993)
18 W.X. Que, X. Hu, Opt. Mater. **27**, 273 (2004)
19 E. Pelletier, F. Flory, Y. Hu, Appl. Opt. **28**, 2918 (1989)
20 D.G. Chen, B.G. Potter, J.H. Simmons, J. Non-Cryst. Solids **178**, 135 (1994)
21 L. Yang, S.S. Saavedra, N.R. Armstrong, H. John, Anal. Chem. **66**, 1254 (1994)
22 P.J. Hughes, A.P. Knights, B.L. Weiss, S. Kuna, P.G. Coleman, S. Ojha, Appl. Phys. Lett. **74**, 3311 (1999)
23 Y. Miyake, H. Nishikawa, E. Watanabe, D. Ito, J. Non-Cryst. Solids **222**, 266 (1997)
24 M. Takahashi, T. Fujiwara, T. Kawachi, A.J. Ikushima, Appl. Phys. Lett. **71**, 993 (1997)
25 H. Hosono, H. Kawazoe, K.I. Muta, Appl. Phys. Lett. **63**, 479 (1993)
26 M.G. Sceat, G.R. Atkins, S.B. Poole, Annu. Rev. Mater. Sci. **23**, 381 (1993)
27 L. Smith, Spectrosc. Acta **16**, 87 (1987)
28 N.B. Colthup, L.H. Daly, S.E. Wiberley, *Introduction to Infrared and Raman Spectroscopy* (Academic, New York, 1964)
29 P.W. Dooley, J. Thøgersen, J.D. Gil, H.K. Haugen, R.L. Brooks, Opt. Commun. **183**, 451 (2000)
30 J. Fernández, R. Balda, A. Mendioroz, M. Sanz, J.-L. Adam, J. Non-Cryst. Solids **287**, 437 (2001)
31 M. Karbowiak, N.M. Edelstein, J. Drożdżyński, J. Luminesc. **104**, 197 (2003)
32 K. Annapurna, R.N. Dwivedi, P. Kundu, S. Buddhudu, Mater. Lett. **57**, 2095 (2003)